

Waveform inversion of shallow seismic refraction data using hybrid heuristic search method

Mika Takekoshi¹ Hiroaki Yamanaka^{1,2}

¹The Interdisciplinary Graduate School of Science and Engineering, Tokyo Institute of Technology, 4259 Nagatsuta, Yokohama, Kanagawa 226-8503, Japan.

²Corresponding author. Email: yamanaka@depe.titech.ac.jp

Abstract. We propose a waveform inversion method for SH-wave data obtained in a shallow seismic refraction survey, to determine a 2D inhomogeneous S-wave profile of shallow soils. In this method, a 2.5D equation is used to simulate SH-wave propagation in 2D media. The equation is solved with the staggered grid finite-difference approximation to the 4th-order in space and 2nd-order in time, to compute a synthetic wave. The misfit, defined using differences between calculated and observed waveforms, is minimised with a hybrid heuristic search method. We parameterise a 2D subsurface structural model with blocks with different depth boundaries, and S-wave velocities in each block. Numerical experiments were conducted using synthetic SH-wave data with white noise for a model having a blind layer and irregular interfaces. We could reconstruct a structure including a blind layer with reasonable computation time from surface seismic refraction data.

Key words: generic algorithm, heuristic search method, seismic refraction data, simulated annealing, waveform inversion.

Introduction

Local site amplification is one of the important factors that determine earthquake ground motion at a site with soft soils. Therefore, detailed subsurface structure is required to predict strong ground motion at such a site during an earthquake. In particular, the lateral variation of subsurface S-wave velocity must be known in order to understand the spatial distribution of earthquake ground motion.

Seismic refraction exploration, using SH waves generated by plank hammering, is one of the most popular methods for deriving a 2D shallow S-wave velocity structure in soft soils (e.g. Kramer, 1996). SH waves are recorded by seismometers deployed in a survey line on the surface. Travel times of the initial phases of the SH wave observed are used to deduce an S-wave velocity model from the surface down to a depth of several tens of metres. Although field operation and analysis in the shallow refraction method is easy and simple, an observed S-wave profile is often too simply interpreted as showing a single subsurface layer over a firm soil, with constant velocities. We sometimes have difficulty in determining a proper soil model from travel time data, if the subsurface contains a blind layer, a velocity reversal, or similar. The existence of these layers cannot be detected in conventional travel time analysis of refracted initial phases (Burger, 1992). Furthermore, travel time data is more or less contaminated with ambient noise, because the initial phases are often small in amplitude when compared with later phases. This also makes it difficult to reconstruct a proper model.

It is possible to overcome these difficulties in travel time analysis by conducting waveform inversion of refraction data, using more information than first-motion travel time data. For example, Pratt et al. (1998) proposed a waveform tomography method, using a gradient-based inversion method with a frequency-domain inversion approach. Waveform tomography was applied in an analysis of shallow seismic data by Gao et al. (2007). Sheng et al. (2006) proposed an early arrival waveform tomography method for refraction data analysis. They applied an

early arrival time window in the time domain to extract data for waveform inversion. Although this method does retrieve more information than is used in travel time inversions, the surface wave parts of the waveform, which are usually sensitive to shallow properties, are not included in their method.

Surface waves contain dispersive features that are dependent on subsurface structure. In particular, the dispersive features are mainly controlled by the S-wave velocity distribution. Therefore, the surface wave dispersion method relies on an alternative approach to using the shallow refraction waveform. In this shallow S-wave profiling method, Rayleigh-wave phase velocities are retrieved from the refraction data (e.g. Hayashi and Suzuki, 2004). Since travel times of the initial S wave are not used in the surface wave method, it is easily applied in noisy urban areas. Although a 2D image of S-wave velocity can be derived from the surface wave method, data must be acquired at many stations for detailed imaging. Furthermore, separation of surface wave modes must be done before the dispersion analysis, if higher-mode surface waves have similar or larger amplitudes to the fundamental modes.

In this study, we propose waveform inversion of shallow seismic refraction data for a 2D inhomogeneous S-wave profile, using a hybrid heuristic inversion algorithm. We use a 2.5D finite-difference calculation to generate the synthetic SH-wave data. Introduction of the heuristic approach in the inversion method enables us to find an optimal model in a complex error space without being trapped in local-minimum solutions (e.g. Yamanaka, 2005). After validation of the method using synthetic data for a simple model, we examine its applicability to a structure that has a blind layer that is hard to detect in travel time inversions.

Method

Forward modelling

For waveform inversion, a forward modelling calculation is required which can generate synthetic SH-seismograms with

true amplitudes in a 2D inhomogeneous soil model from a point source. Since the effects of 3D geometrical spreading must be included in the calculation of the wave field even in 2D media, we use a 2.5D equation of motion for SH waves, with expressions relating stress and velocity as shown by

$$\rho \frac{\partial \dot{v}}{\partial t} = \frac{2}{r} \tau_r + \frac{\partial \tau_r}{\partial r} + \frac{\partial \tau_z}{\partial z} \quad (1)$$

$$\begin{cases} \frac{\partial \tau_r}{\partial t} = \mu \left(\frac{\partial \dot{v}}{\partial r} - \frac{\dot{v}}{r} \right) \\ \frac{\partial \tau_z}{\partial t} = \mu \frac{\partial \dot{v}}{\partial z} \end{cases} \quad (2)$$

The 2.5D equation of motion due to SH waves is numerically solved with a 4th-order (space) and 2nd-order (time) central finite-difference approximation. A staggered finite-difference grid is used in the approximation. Absorbing and sponge buffer boundary conditions are applied at the non-physical boundaries on the bottom, left, and right sides of the finite-difference grid model. The free surface condition is applied on the upper boundary of the model.

Parameterisation

In tomographic inversions, subsurface structure is often parameterised with many cells. In our case of waveform inversions of conventional refraction data, there are a few, up to 10, observation stations recording data from one or two shots at the two ends of a surveying line. It is difficult to reconstruct a tomographic image with many unknown parameters, such as in Figure 1a, from such a small number of observed station data. However, parameterisation with a stack of homogeneous layers having irregular interfaces (Figure 1b) may allow inversion with the small number of station data. However, lateral variation of S-wave velocity is not included in a homogeneous-layers model. Therefore we use a combination of the tomographic-cell (Figure 1a) and homogeneous-layer models (Figure 1b), as can be seen in Figure 1c.

This soil model consists of subsurface layers over a basement having a constant S-wave velocity, which is one of the unknown parameters in the waveform inversion. The subsurface layers above the basement are divided into few layers separated by smooth interfaces. For example, the model in Figure 1c has three subsurface layers. The layer structure of each interface is described with basis functions by Aoi et al. (1995). Using linear combination of a basis function $c_k(x)$ and a coefficient P_k , the interface depth $d(x)$ at location x is written as

$$d(x) = \sum_k^L P_k c_k(x), \quad (3)$$

where L is the number of basis functions. A basis function is defined as

$$c_k(x) = \begin{cases} 1/2 + 1/2 \cos(\pi/\Delta(x - x_k)) & x_{k-1} \leq x \leq x_{k+1} \\ 0 & \text{otherwise} \end{cases}, \quad (4)$$

where Δ and x_k are constants specified in advance. Depth parameters are defined for each interface of a multi-layered model. The unknown parameters to be determined by the inversion are the coefficients P_k in equation 3 that specify the interface shape. In order to model lateral variation of S-wave velocity in subsurface layers, they are divided into blocks as can be seen in Figure 1c. The S-wave velocity in each block is also one of the parameters in the inversion. In order to stabilise the inversion we use smoothing of the S-wave velocity field in each layer with a weighted three-point smoothing operation. For example, the total number of unknown parameters for the model in Figure 1c is 91 (10×3 for P_k and $20 \times 3 + 1$ for S-wave velocities).

The parameterisation of the subsurface structure that we have described can allow us to model soil layers with S-wave variations, separated by geologically discontinuous interfaces. We therefore assume that variations of S-wave velocities are only small in the blocks that belong to the same layer in an inversion. This can be implemented by making the search limits narrow, for S-wave velocities in different blocks in a layer.

Definition of misfit

The misfit function to be minimised in the inversion is defined using observed and theoretical traces. The misfit, E , is calculated from

$$E = \frac{1}{N} \frac{\sum [s^c(t) - s^o(t)]^2}{\sum [s^c(t)]^2}, \quad (5)$$

where $s^o(t)$ and $s^c(t)$ are the observed and calculated waveforms of SH waves. N is the number of stations along the surveying line. In the following numerical experiments, we assume that source wavelet is known before the inversion.

Inversion algorithm

It is expected that the misfit function will have a complex shape. An appropriate initial model is required in least-square-type inversions, because of the local search characteristics. However, we often have no previous knowledge of subsurface structure, especially for shallow near-surface soils. We therefore applied global search algorithms to minimise the misfit function in this study.

Heuristic approaches are among the global search algorithms used in various kinds of geophysical inversion, such as the

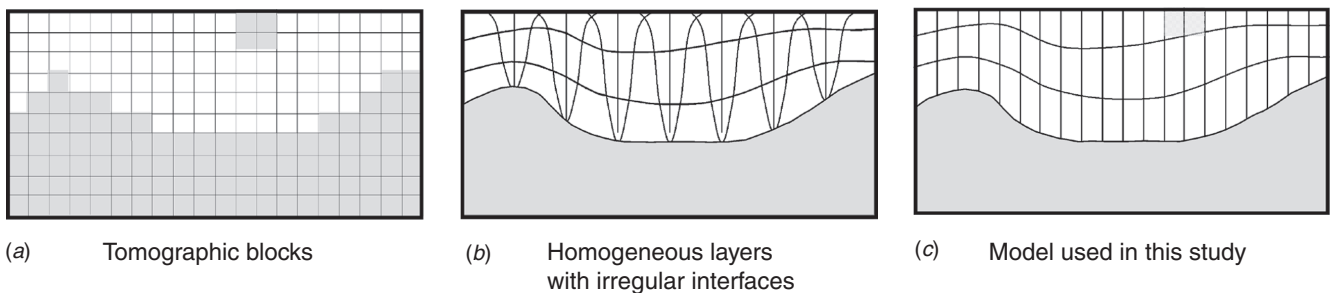


Fig. 1. Model parameterisation with (a) tomographic blocks, (b) homogeneous layers having irregular interfaces defined by summation of trigonometric functions, and (c) combined model with blocks and interfaces, used in this study.

Generic Algorithm (GA) and Simulated Annealing (SA) methods (e.g. Sen et al., 1993). Since heuristic inversion methods often require a significant number of forward calculations, heuristic approaches are less often applied in inversions that require relatively heavy forward computations. We however use the hybrid heuristic method proposed by Yamanaka (2007), because this method is capable of finding an optimal model with less computational effort than required by conventional heuristic algorithms.

The computational flow is shown in Figure 2. The main part of the operation is based on the GA of Yamanaka and Ishida (1996), with three genetic operations of crossover, selection, and mutation. However, a generation-dependent probability of choosing new models from current models (\mathbf{X}) and offspring models (\mathbf{Y}') in the crossover operation is introduced in the hybrid method. The difference, ΔE , between the misfits of the offspring and current models is calculated by

$$\Delta E = E(\mathbf{Y}') - E(\mathbf{X}). \quad (6)$$

We principally select whichever of the parent model or the offspring model has a smaller misfit. If the difference of the two misfits is negative, the offspring model survives in the next generation. However, even when ΔE is positive, there is probability P that an offspring model with a large misfit will still be selected in the next generation. P is defined as

$$P = \exp(-\Delta E/T_k), \quad (7)$$

where T_k is the ‘temperature’ variable at the k -th generation. The temperature is high in the early stages of the computation and becomes gradually lower with increasing generations. The rate of

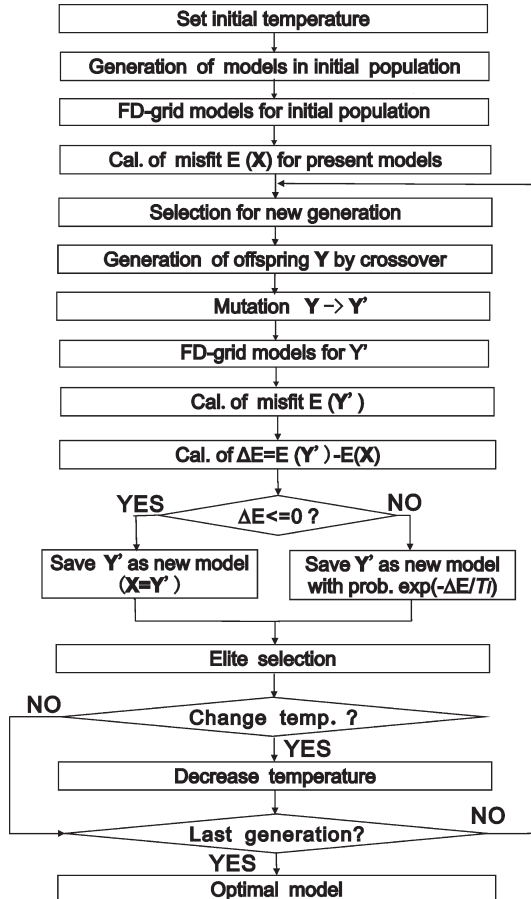


Fig. 2. Computational flow for hybrid heuristic inversion.

decrease of temperature is similar to that in the SA of Yamanaka (2005).

As the temperature decreases, the probability of acceptance works differently in the early and late stages of the search. In the early stage, offspring models with large differences between observed and calculated waveforms can frequently be selected in the next generation, while such models find it hard to survive in later iterations. Only offspring models with smaller misfits than parent models can be chosen in the final stages of the calculation. As is the case with the SA, it is expected that the algorithm can search model space globally and locally because of the generation-dependent acceptance probability. Notice that the hybrid method with infinite temperature works in a similar way to conventional GA. In this study, we also include the elite selection rule of Yamanaka and Ishida (1996), and a real-number coding of the parameters, in the hybrid method. The genetic operations described above are repeated with decreasing temperature until the number of the iterations reaches a given value.

Model and synthetic data

The model used in the numerical experiment has two subsurface layers over a basement with an S-wave velocity of 400 m/s as shown in Figure 3. The thickness of the second subsurface layer is 1 m. This layer cannot be detected with conventional travel time analysis of initial phases, because the layer is too thin, and no refracted waves propagating in the top of the second layer arrive at sites on the surface as initial phases. This kind of thin layer is known as a blind layer in refraction seismology. In addition to the blind layer, there is a slope in the central part of the interfaces in this model.

Synthetic SH waves were calculated at the 10 stations located on the surface of the model. The locations of the stations are shown by triangles in Figure 3. We assumed an explosive point source at the surface. The source time function is assumed to be a Ricker wavelet. In the inversion the source wavelet is known. The grid spacing of the finite-difference model is 0.1 m. Because this grid spacing is sufficiently smaller than the minimum requirements for stable computation, the accuracy of the later phases in calculated wave field is enough to avoid contamination by numerical dispersion. The computed waves are shown in Figure 4. The synthetic data for inversion included theoretical SH waves from forward modelling, and white noise with amplitude 10% of the maximum value of each SH wave.

Inversion results

The heuristic waveform inversion is applied to the synthetic data. The parameters in the inversion are 10 P_k coefficients for each interface, 30 S-wave velocities for blocks in each subsurface

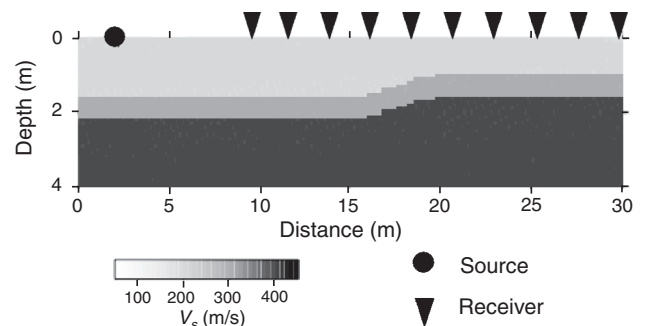


Fig. 3. 2D S-wave velocity model used in our numerical experiment. The circle and triangles indicate the source and stations.

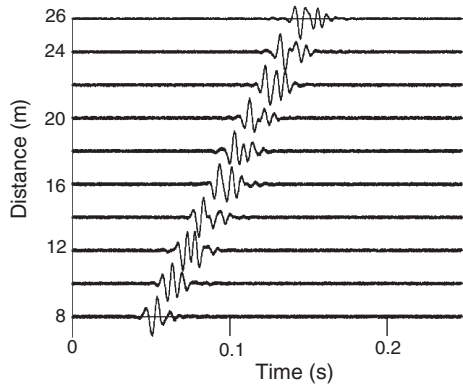


Fig. 4. Synthetic waveform data calculated at the stations on the surface of the model, used as observed data in our numerical experiment. Random noise is included in the synthetic data.

layer, and one S-wave velocity for the basement. In all, 81 parameters are optimised. We first tune the parameters of the heuristic algorithm, such as population size, probabilities of crossover and mutation, and initial temperature. The appropriate combination of parameters, decided from trial runs of the program for several generations, were as follows: population size 20; crossover probabilities 0.7; mutation probability 0.01; and initial temperature 10. The limits of the search spaces for the parameters are tabulated in Table 1.

The first 20 models were randomly generated using a random number generator. Then, the 20 models are modified or replaced through genetic operations, described above. The average and minimum misfits among the 20 models at each generation are shown in Figure 5 with the scheduled temperature decrease also shown. The averaged misfit gradually decreases and almost converges at the 60th generation. This indicates that the many models in each generation are concentrated around the minimum value by means of the hybrid method, acting to search locally. The variations of the S-wave velocities of some of the blocks in the first and second layers are shown in Figure 6. As expected from the average misfit variations in Figure 5, the S-wave velocities are converging to the true values after the 60th generation.

Table 1. Search limits in inversion.

Layer	V_S (m/s)	P_k (m)
1	150–250	0.1–2.0
2	250–350	0.1–1.5
3	350–450	

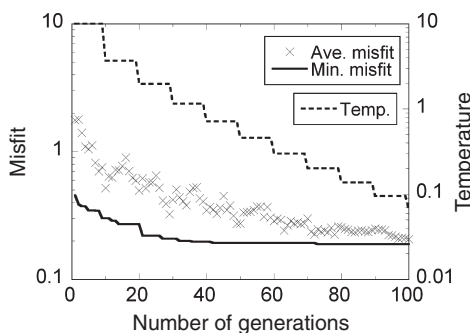


Fig. 5. Variation of the minimum and average misfits at each generation in waveform inversion of the synthetic data in Figure 3 as a function of generation. Temperature decrease is also shown by a broken line.

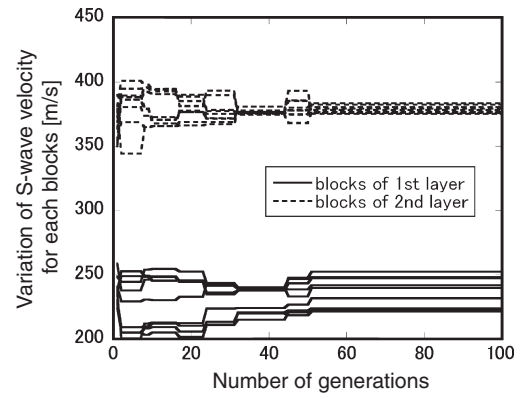


Fig. 6. Variation of S-wave velocities in the blocks in the first and second layers at each generation in the waveform inversion of the synthetic data in Figure 3.

Since many random numbers are used in heuristic search methods, including in the hybrid method used in this study, the variations in misfits and parameters described above are more or less dependent on the random numbers used in each execution of the program. We therefore conducted 10 inversions with different initial values of the random number generator used in the program. The minimum misfits derived at each generation in the 10 inversions are shown in Figure 7 together with their averaged values. It is noted that the minimum misfits in the figure differed from each other in the 10 inversions, because of different

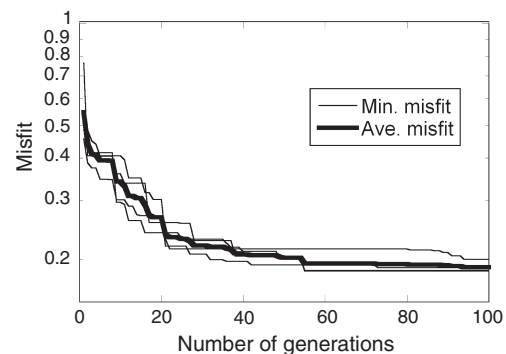


Fig. 7. Variation of the minimum misfits (thin lines) at each generation in 10 inversions of the synthetic data in Figure 3, each with different initial values of the random number generator used in the program. The average value of the 10 minimum misfits at each generation is also shown by a thick line.

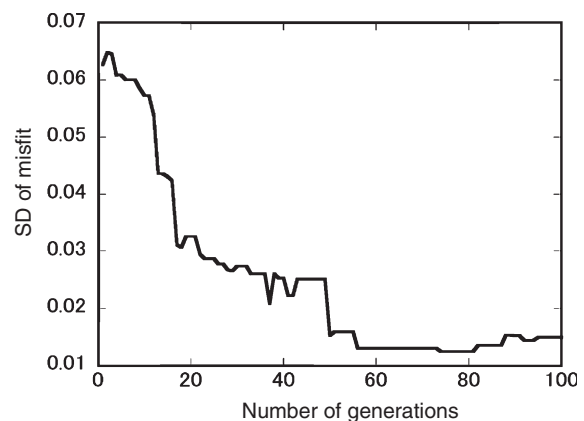


Fig. 8. Variation in standard deviation of the minimum misfits at each generation for 10 inversions of the synthetic data in Figure 3, with different initial values of the random number generator.

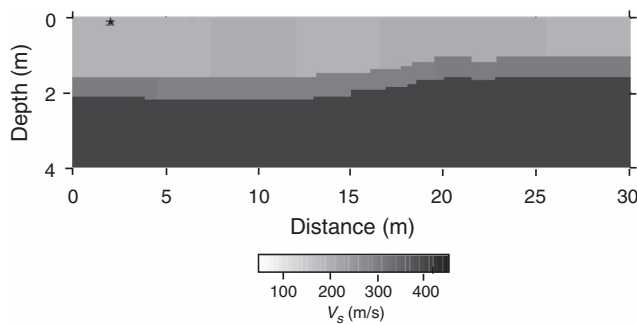


Fig. 9. S-wave velocity model from waveform inversion of the synthetic data in Figure 3. The S-wave velocities and interface depth coefficients are derived from averaging model parameters of 10 optimal models from 10 inversions with different initial values of the random number generator.

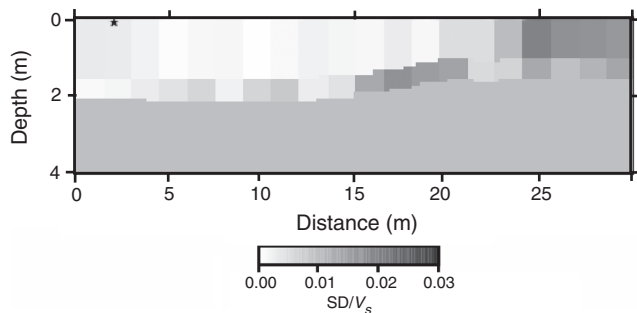


Fig. 10. Distribution of standard deviation of the S-wave velocities of the blocks for the 10 optimal models from 10 inversions with different initial values of the random number generator.

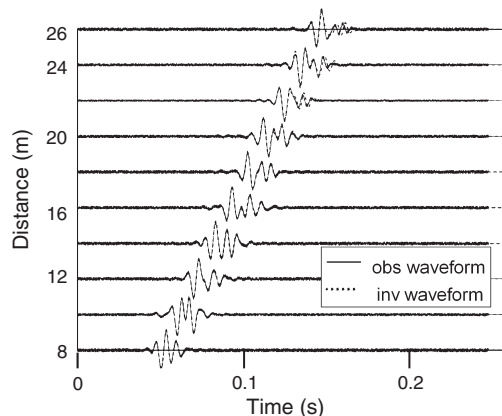


Fig. 11. Comparison of calculated SH waves for the inverted model in Figure 9 with synthetic observed data.

details of the convergence with increasing generations. The variation of the standard deviation of the minimum misfits is shown in Figure 8. The standard deviation becomes small at the 50th generation indicating stability of the inverted results regardless of the initial values of the random number generator.

The model parameters for the models with minimum misfits in each of the 10 inversions are averaged to determine the final inverted results. According to the idea of acceptable solutions (Yamanaka, 2007) all of the models with misfits of less than a threshold value are used in the averaging. We used a threshold 1.5 times larger than the minimum misfit among the all misfits examined in the 10 inversions. The final model is depicted in Figure 9. The blind layer and the slope of the interfaces have been well reconstructed in the inverted model. The thickness to the

basement is less than in the true model near the source. This is due to low sensitivity to the structure near the source, because the observed motions are obtained at stations at a distance of more than 10 m from the source. The standard deviations of the S-wave velocities for the blocks in the acceptable solutions are shown in Figure 10. Since most of the standard deviation for the S-wave velocities is less than 1%, they have converged to the true values. The synthetic seismograms for the inverted model are compared with those for the synthetic observed data in Figure 11. The waveforms for the inverted model are almost identical with synthetic seismograms.

Conclusions

A hybrid heuristic waveform inversion method is proposed to retrieve a 2D S-wave velocity profile from shallow seismic refraction data. The subsurface structure is parameterised with irregular-shaped interfaces between subsurface layers that contain lateral S-wave velocity variations. The interface depth is expressed by linear summation of mathematical basis functions. The inhomogeneity in the S-wave velocity in each layer is modelled by introducing blocks having different S-wave velocities. The effectiveness of the method is demonstrated by inversion of synthetic SH wave data, observed at the surface of a 2D shallow soil model having a blind layer over the basement. The true model could be well reconstructed by the waveform inversion.

Acknowledgments

The comments from two reviewers are appreciated to improve the manuscript. The authors acknowledge financial support from Japan Ministry of Education, Culture, Sport, Science, and Technology (MEXT).

References

- Aoi, S., Iwata, T., Irikura, K., and Sanchez-Sesma, F. J., 1995, Waveform Inversion for Determining the Boundary Shape of a Basin Structure: *Bulletin of the Seismological Society of America*, **85**, 1445–1455.
- Burger, H. R., 1992, Exploration geophysics of the shallow subsurface: Prentice-Hall Inc., 95–101.
- Gao, F., Levander, A., Pratt, R. G., Zelt, C. A., and Fradelizio, G.-L., 2007, Waveform tomography at a groundwater contamination site: Surface reflection data: *Geophysics*, **72**, G45–G55. doi: 10.1190/1.2752744
- Hayashi, K., and Suzuki, H., 2004, CMP cross-correlation analysis of multi-channel surface-wave data: *Exploration Geophysics*, **35**, 7–13. doi: 10.1071/EG04007
- Kramer, S. L., 1996, Geotechnical Earthquake Engineering: Prentice-Hall Inc.
- Pratt, R. G., Shin, C., and Hicks, G. J., 1998, Gauss-Newton and full Newton methods in frequency seismic waveform inversion: *Geophysical Journal International*, **133**, 341–361. doi: 10.1046/j.1365-246X.1998.00498.x
- Sen, M. K., Bhattacharya, B. B., and Stoffa, P. L., 1993, Nonlinear inversion of resistivity sounding data: *Geophysics*, **58**, 496–507. doi: 10.1190/1.1443432
- Sheng, J., Leeds, A., Buddensiek, M., and Schuster, G. T., 2006, Early arrival waveform tomography on near-surface refraction data: *Geophysics*, **71**, U47–U57. doi: 10.1190/1.2210969
- Yamanaka, H., and Ishida, H., 1996, Application of genetic algorithms to an inversion of surface-wave dispersion data: *Bulletin of the Seismological Society of America*, **86**, 436–444.
- Yamanaka, H., 2005, Comparison of performance of heuristic search methods for phase velocity inversion in shallow surface wave methods: *Journal of Environmental & Engineering Geophysics*, **10**, 163–173. doi: 10.2113/JEEG10.2.163
- Yamanaka, H., 2007, Inversion of surface-wave phase velocity using hybrid heuristic search method: *Butsuri Tansa*, **60**, 265–275.

ハイブリッドヒューリスティック法による 表層地盤を対象にした屈折法地震探査データの波形逆解析

竹越美佳¹・山中浩明¹

¹ 東京工業大学 大学院総合理工学研究科

要旨: 板たたきなどの震源を用いた屈折法地震探査では、一般的にSH波の初動走時に着目して表層10 m程度までのS波速度構造が推定されている。初動走時に基づく手法では、ノイズが大きい地域では走時の読み取りが難しいことや複雑な地盤構造では適切な結果が得られないこと等の問題点がある。本研究では、表層地盤を対象にした屈折法に基づく地震探査の波形データの逆解析によって2次元地盤構造モデルを推定する方法を提案している。順解析では、SH波の2.5次元運動方程式を差分法によって近似して地表での波形を計算した。2次元地盤構造のモデル化では、各境界面深度を基底関数の線形和として表現し、各層内部をブロックに分割し、速度不均質を導入した。基底関数の係数とブロックのS波速度をモデルパラメータとして、それらを観測波形と計算波形の差を最小化するようにハイブリッドヒューリスティック法に基づいて推定した。数値実験では、ブラインド層を含む表層地盤モデルに対する順計算により得られた波形にホワイトノイズを加えたものを擬似的な観測データとして逆解析を行った。その結果、走時解析では検出できない層を含めてS波速度構造モデルを再構築することができ、本手法の有効性を確認した。

キーワード: 波形逆解析, 屈折法地震探査, ヒューリスティック探索, 遺伝的アルゴリズム, 焼きなまし法

하이브리드 발견적 탐색기법을 이용한 천부 굴절법 자료의 파형역산

Mika Takekoshi¹, Hiroaki Yamanaka¹

¹ 동경공업대학교 공학대학원

요약: 본 연구에서는 천부 토양층의 2차원 불균질 S파 단면을 결정하기 위해 천부 굴절법 탐사로부터 얻은 SH파 자료에 대한 파형역산 기법을 제안한다. 2차원 매질에서 SH파의 전파를 모사하기 위해 2.5차원 파동 방정식을 사용한다. 합성탄성파를 계산하기 위해 공간축으로 4차, 시간축으로 2차 근사한 staggered grid 유한차분법을 사용하여 파동 방정식을 푼다. 계산된 파형과 측정 파형의 잔여오차로 정의되는 목적함수를 하이브리드 발견적 탐색기법에 의해 최소화한다. 2차원 지하구조 모형은 각기 다른 심도 경계면을 갖는 블록과 블록 내부의 S파 속도에 의해 매개화한다. 수치실험은 암영층과 불규칙한 경계를 갖는 모델에 대해 백색잡음을 추가한 합성 SH파 자료를 이용하여 수행하였다. 지표 굴절법 자료로부터 암영층을 포함한 구조를 적절한 계산시간 내에 영상화할 수 있었다.

주요어: 파형역산, 탄성파 굴절법 자료, 발견적 탐색기법, 유전자 알고리즘, 담금질모사법